Proving Asymptotic Stability of a Walking Cycle for a Five DOF Biped Robot Model

J. W. Grizzle, Gabriel Abba and Franck Plestan

Abstract

To date, for the case of a biped robot with a torso, none of the various control approaches have produced a closed-loop system with provable stability properties. Since regular walking can be viewed as a periodic solution of the robot model, the method of Poincaré sections is the natural analysis tool. However, due to the complexity of the associated dynamic models, this approach has only been successfully carried out for Raibert's one-legged-hopper [18], [5], [8], and a biped robot without a torso [32], [10], [30]. In a recent paper [11], the authors have developped a control strategy that leads to a straightforward stability analysis for a class of under actuated biped models. The primary goal of this paper is to illustrate this new control and analysis approach on a five degree of freedom biped model.

I. Introduction

The biped robot used in this study is depicted in Figure 1: it consists of a torso, hips, and two legs of equal length, with no ankles and no knees. It thus has five degrees of freedom. Two torques, u_1 and u_2, are applied between the torso and the stance leg, and the torso and the swing leg, respectively, so the system is under actuated for any gait. The angular coordinates and the disposition of the masses of the legs, hips and torso are all shown in Figure 1. In particular, note that θ_1 parameterizes the stance leg, θ_2 the swing leg, θ_3 the torso, positive angles are computed clockwise with respect to the indicated vertical lines, and all masses are lumped.

At its most basic level, walking consists of two things [25]: posture control, that is, maintaining the torso in a semi-erect position, and swing leg advancement, that is, causing the swing leg to come from behind the stance leg, pass it by a certain amount, and prepare for contact with the ground. This motivates the direct control of the angles θ_3 (describing the torso) and θ_2 (describing the swing leg). By far, the most common approach to control in the multi-ped literature is through the tracking of pre-computed reference trajectories [33], [24], [9], [6]. That is, in the context of the robot model investigated here, the first step of the control design would be to determine functions of time $\theta_2(t)$ and $\theta_3(t)$ that express a desired behavior of the robot. Then, standard control techniques would be employed to induce "asymptotic" tracking of these trajectories [26]. The resulting closed-loop system is nonlinear, time-varying (due to the time-dependent reference trajectories) and very difficult to analyze.

On a periodic orbit corresponding to a normal walking motion, it is clear that the horizontal motion of the hips is monotonically strictly increasing. For the biped of Figure 1, this is equivalent to $\theta_1(t)$ strictly increasing over each step of the walking cycle. Thus, for any desired trajectories $\theta_2(t)$ and $\theta_3(t)$ that express (encode) a desired walking pattern for the biped, it is therefore reasonable to assume that the corresponding trajectory for θ_1 has the property that $\theta_1(t)$ is strictly monotonic. It follows that $\theta_2(t)$ and $\theta_3(t)$ can each be re-parameterized in terms of θ_1. That is, without loss of generality, it can be supposed that $\theta_3(t) = \eta_1(\theta_1(t))$ and $\theta_2(t) = \eta_2(\theta_1(t))$, for some functions η_i. The "behavior" of walking can thus be "encoded" into the dynamics of the robot by defining outputs

$$y := \begin{bmatrix} y_1 \\ y_2 \end{bmatrix} := \begin{bmatrix} h_1(\theta) \\ h_2(\theta) \end{bmatrix} := \begin{bmatrix} \theta_3 - \eta_1(\theta_1) \\ \theta_2 - \eta_2(\theta_1) \end{bmatrix}, \tag{1}$$

with the control objective being to drive the outputs to zero.

Of course, the idea of building in a dynamic behavior of a system through the judicious definition of a set of outputs, which when nulled yields a desirable internal behavior, is not novel in control [15] nor walking robots [17], [13], [3], [16], [22], [28], [8]. However, it is interesting to note that this idea, which seems to be an essential step for *proving* anything about the trajectories of the closed-loop system, has only been used to analytical advantage in the monoped (one-legged hopper) literature. This seems to be due to the fact that realistic, analytically tractable models of the hopper exist, and the associated Poincaré return map can be analyzed in considerable detail [3], [28], [8]. This has led to the determination of *sampled-data* control laws (sampling is done synchronously with impact events) that lead to *explicit*, *low-dimensional* tests for asymptotic stability of a periodic orbit.

Even for the simple biped model considered in this work, analyzing the return map would be a formidable task, and doing this for a more complete model of a robot with knees is simply unthinkable at the present time. Here, a completely different approach to obtaining an *explicit*, *low-dimensional* test for asymptotic stability of a periodic orbit will be illustrated [11]. The control design will be done in continuous-time, and computed directly from the robot model

J.W. Grizzle is with the Control Systems Laboratory, Electrical Engineering and Computer Science Department, University of Michigan, Ann Arbor, MI 48109-2122, Tel: (734)-763-3598, FAX: (734)-763-8041, Email: grizzle@umich.edu.
G. Abba and F. Plestan are with GRAVIR-LSIIT, ENSPS-Université Louis Pasteur-CNRS, Blvd. Sébastien Brant, 67400 Illkirch-Graffenstaden, France, Tel: (0)3-88-65-50-87, Fax: (0)3-88-65-54-89, Email: {Gabriel.Abba,Franck.Plestan}@ensps.u-strasbg.fr
Corresponding author: Franck Plestan

and the choice of outputs to be controlled. In the spirit of [3], [28], it will also have a dead-beat character, and will lead to a stability test based on the computation of a map from a subset of $\mathbb{R}$ to itself; this will be achieved with continuous, finite-time feedback controllers [12], [1], [2].

For the sake of completeness, it is noted that other control methods have been investigated that do not rely on pre-computed reference trajectories for the angular positions; these include controlling energy, angular momentum, and others [27], [10], [19], [25]. None of these have led to stability proofs for a biped with a torso.

II. Biped model

It is assumed that the walking cycle takes place in the (sagittal) plane. It is further assumed that the walking cycle consists of successive phases of single support, with the transition from one leg to another taking place in an infinitesimal length of time [29], [7]. This assumption entails the use of a rigid model to describe the impact of the swing leg with the ground. The model of the biped robot thus consists of two parts: the differential equations describing the dynamics of the robot during the swing phase, and an impulse model of the contact event.

During the swing phase of the motion, the stance leg is modeled as a pivot, and thus there are only three degrees of freedom. In order for the swing leg to move without touching the ground until the desired moment of contact, the idea of [21] is adopted here: the swing leg is assumed to move out of the plane of forward motion, and into the frontal (coronal) plane. This allows the swing leg to clear the ground and be posed in front of the stance leg (think of a person with a cast over their knee). It will be further assumed that the swing leg is designed to renter the plane of motion when the angle of the stance leg attains a given value, θ_1^d. Alternate means of achieving leg clearance in rigid legged robots are discussed in [21], [7].

The dynamic model of the robot between successive impacts is easily derived using the method of Lagrange [31], and results in a standard second order system

$$D(\theta)\ddot{\theta} + C(\theta,\dot{\theta})\dot{\theta} + G(\theta) = Bu, \tag{2}$$

where $u = (u_1, u_2)'$, and $\theta = (\theta_1, \theta_2, \theta_3)'$. The matrices D, C, G and B are deduced from the Lagrangian formulation of the dynamics (given in the Appendix). The second order system (2) is written in state space form by defining

$$\dot{x} := \frac{d}{dt}\begin{bmatrix} \theta \\ \omega \end{bmatrix} = \begin{bmatrix} \omega \\ D^{-1}(\theta)\left(-C(\theta,\omega)\omega - G(\theta) + Bu\right) \end{bmatrix} =: f(x) + g(x)u. \tag{3}$$

The state space for the system is taken as $\mathcal{X} := \{x := (\theta', \omega')' \mid \theta \in M,\ \omega \in \mathbb{R}^3\}$, where $M = (-\pi, \pi)^3$.

The second part of the model involves the impact between the swing leg and the ground. This is modeled as a contact between two rigid bodies, and the standard model from [14] is used. The premises underlying this model are that: (a) the impact takes place over an infinitesimally small period of time; (b) the external forces during the impact can be represented by impulses; (c) impulsive forces may result in an instantaneous change (i.e., a discontinuity) in the velocities of the generalized coordinates, but the positions remain continuous; and (d) the torques supplied by the actuators are not impulsional. If it is further assumed that the contact of the swing leg with the ground results in no rebound and no slipping of the swing leg, and the stance leg naturally lifting from the ground without interaction, an expression for x^+, the position and velocity just after the impact, can be computed from x^-, the position and velocity just before the impact [14]. Finally, since the coordinate definition of the swing phase model assumes that θ_1 corresponds to the stance leg and θ_2 to the swing leg, it is necessary to do a coordinate transformation after the impact, which amounts to swapping the first two position coordinates, and the first two velocity coordinates, respectively. The final result is expressed as $\Delta : S \to \mathcal{X}$, where

$$S := \{(\theta,\omega) \in \mathcal{X} \mid \theta_1 = \theta_1^d\}, \tag{4}$$

and

$$x^+ = \Delta(x^-) := \begin{bmatrix} \theta_2^- \\ \theta_1^- \\ \theta_3^- \\ \omega_2^+(x^-) \\ \omega_1^+(x^-) \\ \omega_3^+(x^-) \end{bmatrix}; \tag{5}$$

ω_1^+, ω_2^+ and ω_3^+ are specified in the Appendix. It is noted in passing that S can be expressed as the level set of a function $H : \mathcal{X} \to \mathbb{R}$. Define $H(x) = \theta_1^d - \theta_1$, so that $S := \{(\theta,\omega) \in \mathcal{X} \mid H(x) = 0\}$. Moreover, it can be easily checked that for each point $s \in S$, $\frac{\partial H}{\partial x}(s) \neq 0$. This implies that S is a smooth embedded submanifold of $\mathcal{X}$ [15]. In the Appendix, it is seen that Δ is a smooth function of its arguments.

III. Controller Design

The simplest version of posture control is to maintain the angle of the torso at some constant value, say θ_3^d, while the simplest version of swing leg advancement is to command the swing leg to behave as the mirror image [4] of the stance leg, that is, $\theta_2 = -\theta_1$. These correspond to $\eta_1(\theta_1) = \theta_3^d$ (a constant) and $\eta_2(\theta_1) = -\theta_1$:

$$y := \begin{bmatrix} y_1 \\ y_2 \end{bmatrix} := \begin{bmatrix} h_1(\theta) \\ h_2(\theta) \end{bmatrix} := \begin{bmatrix} \theta_3 - \theta_3^d \\ \theta_2 + \theta_1 \end{bmatrix}; \tag{6}$$

other choices will be investigated in a later section.

Since the system (3) comes from the second order model (2), and the outputs (6) only depend upon θ, it follows that the relative degree of each output component is either two or infinite. Direct computation gives that [15], [20], [23]

$$\ddot{y} = L_f^2 h(x) + L_g L_f h(x) u \tag{7}$$

and the determinant of the decoupling matrix, $L_g L_f h$, is further computed to be

$$-r\left(rM_H + rm + rM_T + lM_T\cos(\theta_1 - \theta_3)\right).$$

Thus, the decoupling matrix is invertible for all $x \in \mathcal{X}$ as long as $0 < lM_T < r(m + M_T + M_H)$, which imposes a very mild constraint on the position of the center of gravity of the upper body of the robot in relation to the length of its legs. This leads to the following hypothesis.

Hypothesis CH1): The decoupling matrix is globally invertible.

From now on, it is supposed that CH1 is met. Therefore, stabilizing dynamics for the output of system (3) can be assigned. The easiest way to do this is through the method of computed torque: first decouple the system [15], [23], [20] and then impose a desired dynamic response. In preparation for doing this, note that $\Phi : M \to \mathbb{R}^3$ by

$$\Phi(\theta) := \begin{bmatrix} y_1 \\ y_2 \\ \theta_1 \end{bmatrix} = \begin{bmatrix} \theta_3 - \theta_3^d \\ \theta_1 + \theta_2 \\ \theta_1 \end{bmatrix} \tag{8}$$

is a global change of coordinates. With this coordinate transformation, and upon defining

$$v := L_f^2 h + L_g L_f h u, \tag{9}$$

the system can be written in the decoupled-form

$$\begin{bmatrix} \ddot{y} \\ \ddot{\theta}_1 \end{bmatrix} = \begin{bmatrix} v \\ \zeta_0(y, \dot{y}, \theta_1, \dot{\theta}_1) + \zeta_1(y, \dot{y}, \theta_1, \dot{\theta}_1) v \end{bmatrix}. \tag{10}$$

The next step is to impose a continuous feedback $v = v(y, \dot{y})$ on (10), and thus on (3), so that the pair of double integrators $\ddot{y} = v$ is *globally finite-time stabilized* [1], [2]. The purpose of using a finite-time controller is that it will collapse the image of the Poincaré return map to a one-dimensional set, and lead to a tractable analysis condition.

Hypotheses: The closed-loop pair of double integrators, $\ddot{y} = v(y, \dot{y})$, satisfies the following conditions:

CH2) solutions globally exist on $\mathbb{R}^4$, and are unique;

CH3) solutions depend continuously on the initial conditions;

CH4) the origin is globally asymptotically stable, and convergence is achieved in finite time;

CH5) the settling time function[1], $T_{set} : \mathbb{R}^4 \to \mathbb{R}$ by

$$T_{set}(y_0, \dot{y}_0) := \inf\{t > 0 \mid (y(t), \dot{y}(t)) = (0,0),\ (y(0), \dot{y}(0)) = (y_0, \dot{y}_0)\}$$

depends continuously on the initial condition, $(y_0, \dot{y}_0)$.

Hypotheses CH2-CH4 correspond to the definition of finite-time stability [12], [1]; CH5 is also be needed in the technical analysis of [11], but is not implied by CH2-CH4 [2]. These requirements rule out traditional sliding mode control, with its well-known discontinuous action. A means of meeting these four objectives is provided in [1], [2]; see Section V. Let $\psi_i(x_1, x_2)$, $i = 1, 2$, be *any* feedbacks for the pair of double integrators in (10) so that, with

$$v := \Psi(y, \dot{y}) := \begin{bmatrix} \psi_1(y_1, \dot{y}_1) \\ \psi_2(y_2, \dot{y}_2) \end{bmatrix}, \tag{11}$$

[1] That is, the time it takes for a solution initialized at $(y_0, \dot{y}_0)$ to converge to the origin. The terminology is taken from [1].

CH2-CH5 are satisfied for $\ddot{y} = v$. Define a feedback on (3) by

$$u(x) := (L_g L_f h(x))^{-1} \left(\Psi(h(x), L_f h(x)) - L_f^2 h(x) \right), \tag{12}$$

and denote the right-hand side of the closed-loop by

$$f_{cl}(x) := f(x) + g(x)u(x). \tag{13}$$

Finally, define

$$T_{set}^{cl}(x) := T_{set}(h, L_f h). \tag{14}$$

It follows that $T_{set}^{cl}(x)$ is a continuous function of x.

IV. Method of Poincaré for Finite-Time Control

This section provides a summary of the method of Poincaré, specialized for the case of finite-time control of the biped model with rigid impacts, assuming that CH1-CH5 hold. The mathematical justification of the results is given in [11]. The reader wishing only to see the application may skip to the next section.

Let $\varphi^{f_{cl}}(t, x_0)$ denote the solution of (13) at time t for the initial condition x_0 at time $t_0 = 0$. Define the *time to impact* function, $T_I : \mathcal{X} \to \mathbb{R} \cup \{\infty\}$, by

$$T_I(x_0) := \begin{cases} \inf_{t \geq 0}\{\varphi^{f_{cl}}(t, x_0) \in S\} & \text{if } \exists\ t \text{ such that } \varphi^{f_{cl}}(t, x_0) \in S \\ \infty & \text{otherwise} \end{cases} \tag{15}$$

It can be shown that T_I is continuous at points x_0 where $0 < T_I(x_0) < \infty$ and $L_f H(\varphi^{f_{cl}}(T_I(x_0), x_0)) \neq 0$ (points where an impact takes place in finite time, and the impact is transversal to S). From this, it can be shown that $\tilde{S} := \{x \in S \mid 0 < T_I(\Delta(x)) < \infty \text{ and } L_f H(\varphi^{f_{cl}}(T_I(\Delta(x)), \Delta(x))) \neq 0\}$ is an open subset of S; in words, $\tilde{S}$ is the set of points in S which, after the application of the impact model, give rise to a trajectory of the swing phase model that will have another (transversal) impact with S. The *Poincaré return map* is then defined by $P : \tilde{S} \to S$ by

$$P(x) := \varphi^{f_{cl}}(T_I(\Delta(x)), \Delta(x)), \tag{16}$$

and can be shown to be well-defined and continuous.

The next step is to exploit the finite-time convergence property of the controller. The internal dynamics of the system (3) compatible with the output (6) being identically zero is called the zero dynamics [15], and the state space on which the zero dynamics evolves is called the zero dynamics manifold. For the biped model under study, the zero dynamics manifold is computed from (10) to be

$$Z = \left\{ (\theta, \omega) \in \mathcal{X} \mid \theta_3 = \theta_3^d,\ \theta_1 + \theta_2 = 0,\ \omega_3 = 0,\ \omega_1 + \omega_2 = 0,\ -\pi < \theta_1 < \pi,\ \omega_1 \in \mathbb{R} \right\}. \tag{17}$$

Next, the set $\hat{S} := \{x_0 \in \tilde{S} \mid T_{set}^{cl}(x_0) < T_I(x_0) < \infty\}$ (points were the convergence time of the controller is less than the time of a walking cycle) is an open subset of $\tilde{S}$. It follows that $P : \hat{S} \to S \cap Z$. In terms of the original coordinates (θ, ω) of the robot,

$$S \cap Z = \left\{ (\theta, \omega) \in \mathcal{X} \mid \theta_3 = \theta_3^d,\ \theta_1 + \theta_2 = 0,\ \omega_3 = 0,\ \omega_1 + \omega_2 = 0,\ \theta_1 = \theta_1^d,\ \omega_1 \in \mathbb{R} \right\},$$

a one-dimensional (embedded) submanifold of $\mathcal{X}$. Define

$$\rho : \hat{S} \cap Z \to S \cap Z \text{ by } \rho(x) := P(x). \tag{18}$$

THEOREM 1 (Method of Poincaré for Finite-Time Control [11]) Consider the biped robot model of Section II. Define outputs such that Hypothesis CH1 is met. Suppose that a continuous, finite-time stabilizing feedback is applied, and that Hypotheses CH2-CH5 are met. Define Z, $\hat{S}$ and ρ as above. Then,

1. $x^* \in \hat{S} \cap Z$ gives rise to a periodic orbit of the closed-loop biped model if, and only if, $\rho(x^*) = x^*$.
2. $x^* \in \hat{S} \cap Z$ gives rise to a stable (resp., asymptotically stable) periodic orbit of the closed-loop biped model if, and only if, x^* is a stable (resp., asymptotically stable) equilibrium point of ρ.

V. Numerical illustration

Consider the biped model with the following values of the parameters:

$$m = 5 \quad M_H = 15 \quad M_T = 10 \quad r = 1 \quad l = 0.5$$

corresponding to the mass of the legs, the mass of the hips, the mass of the torso, the length of the legs and the distance between the center of mass of the hips and the center of mass of the torso. The units are kilograms and meters. With the outputs defined as in (6), Hypothesis CH1 is met. Suppose that the desired inclination angle of the torso is $\theta_3^d = \pi/6$ and that impact occurs with the walking surface when $\theta_1^d = \pi/8$. In the feedback (12), suppose that

$$\Psi(x) := \begin{bmatrix} \frac{1}{\epsilon^2}\psi_\alpha(y_1, \epsilon\dot{y}_1) \\ \frac{1}{\epsilon^2}\psi_\alpha(y_2, \epsilon\dot{y}_2) \end{bmatrix} \tag{19}$$

is used, with $\epsilon = 0.1$ and $\alpha = 0.9$, where $\psi_\alpha(x_1, x_2)$ is given by [1]

$$\psi_\alpha(x_1, x_2) := -\text{sign}(x_2)|x_2|^\alpha - \text{sign}(\phi_\alpha(x_1, x_2))|\phi_\alpha(x_1, x_2)|^{\frac{\alpha}{2-\alpha}}, \tag{20}$$

where $\phi_\alpha(x_1, x_2) := x_1 + \frac{1}{2-\alpha}\text{sign}(x_2)|x_2|^{2-\alpha}$. The parameter $\epsilon > 0$ allows the settling time of the controller to be adjusted. With this feedback, CH2-CH5 hold [1], [2].

To determine if this choice of parameters results in an asymptotically stable orbit that is transversal to $\hat{S}$, that is, the orbit is transversal to S and the finite-time stabilizing feedback has had enough time to converge over the walking cycle, the function ρ of Theorem 1 must evaluated. This is conveniently done as follows. Define $\sigma : I\!R \to \hat{S} \cap Z$ by $\sigma(\omega_1^-) := (\theta_1^d, -\theta_1^d, \theta_3^d, \omega_1^-, -\omega_1^-, 0)$, where ω_1^- denotes the angular velocity of the stance leg just before impact. Define $\lambda := \sigma^{-1} \circ \rho \circ \sigma$. A straightforward procedure for evaluating λ on the basis of a simulation model of the closed-loop system is now given.

Numerical Procedure to Test for Walking Cycles via the Method of Poincaré:

1) For a point $\omega_1^- > 0$, compute $x^- := \sigma(\omega_1^-)$, the position of the robot just before impact (the restriction to positive velocities corresponds to the robot walking from left to right).

2) Apply the impact model to x^-, that is, compute $x^+ := \Delta(x^-)$, via (5).

3) Use x^+ as the initial condition in (13), the robot in closed loop with the controller, and simulate until one of the following happens:

a) there exists a time $T > 0$ where $\theta_1(T) = \theta_1^d$; then, if T is greater than the settling time of the controller (in other words, the output y is identically zero), then $x^+ \in \hat{S} \cap Z$, and $\lambda(\omega_1^-) = \omega_1(T)$; else, $x^+ \notin \hat{S} \cap Z$, and $\lambda(\omega_1^-)$ is undefined at this point.

b) there does not exist a $T > 0$ such that $\theta_1(T) = \theta_1^d$ (which is normally detected by one of the angles exceeding $\pm\pi$ during the simulation); in this case, it is also true that $x^+ \notin \hat{S} \cap Z$, and $\lambda(\omega_1^-)$ is undefined at this point.

Figure 2 displays the function λ; it also displays the related function $\delta\lambda(\omega_1^-) := \lambda(\omega_1^-) - \omega_1^-$, which represents the change in velocity over successive cycles, from just before an impact to just before the next one. It is seen that λ is undefined for ω_1^- less than approximately 1.32 radians/second (for initial ω_1^- less than this value, the robot fell backwards). The plot was truncated at 2 radians/second because nothing interesting occurs beyond this point (except an upper bound on its domain of existence will eventually occur due to the controller not having enough time to settle over one walking cycle). A fixed point occurs at approximately 1.6 radians/second, and, from the graph of λ, it clearly corresponds to an asymptotically stable walking cycle. This is supported by Figure 3, which depicts the limit cycle projected onto $(\theta_1, \omega_1, \omega_3)$.

To illustrate the role played by the inclination of the torso, suppose that θ_3^d is reduced by half to $\pi/12$. Figure 4 displays λ and $\delta\lambda$ for this case. It is seen that there is no fixed point, and hence no periodic orbit that is transversal to $\hat{S}$. Simulations also support this conclusion, but are not reported here for reasons of space. For a robot without knees or ankles, the driving force for walking comes from the inclination of the torso, which couples in the force of gravity.

VI. Approximate minimization of energy consumption over an asymptotically stable walking cycle

The goal of this section is to illustrate how Theorem 1 can be used to improve the choice of the output functions made in (6), in order to use less energy over a walking cycle, and/or to reduce the magnitude of the required torques. The feedback solution computed in the previous section uses large torques (on the order of 800 Nm) because the feedback design did not try to exploit the natural evolution of the robot. Consider the robot model with parameters and controller as selected in Section V. Let $h_1^a(x) = \theta_3 - \eta_1^a(\theta_1)$ and $h_2^a(x) = \theta_2 - \eta_2^a(\theta_1)$, where each η_i^a is a polynomial in θ_1, and $a = (a_1, \ldots, a_N)$ is a vector of parameters. The objective is to choose the parameter vector a in such a manner that the feedback

$$u(t) := (L_g L_f h^a(x(t)))^{-1} \left(\Psi(x(t)) - L_f^2 h^a(x(t))\right), \tag{21}$$

with Ψ as in (19), will induce an asymptotically stable walking cycle, and result in lower energy consumption (and hopefully, lower torques) over the walking cycle than the feedback based on (6).

From Theorem 1, a necessary condition for the existence of an asymptotically stable walking cycle is the existence of a pre-impact velocity ω_1^- such that $\lambda(\omega_1^-) > \omega_1^-$. For the biped model as used in Section V, $\lambda(1.55) = 1.574 > 1.55$. Let $\hat{\omega}_1^- := 1.55$. Define a cost function by

$$\hat{J}(a) := \int_0^{\hat{T}} u_1^2(t) + u_2^2(t)dt, \tag{22}$$

where, $\hat{T} := \min\{T_I(\Delta \circ \sigma(\hat{\omega}_1^-)), 2\}$ and $u(t)$ is the result of applying (21) to (13), with initial condition $x_0 := \Delta \circ \sigma(\hat{\omega}_1^-)$ (the upper-bound on $\hat{T}$ is to keep the cost finite for initial conditions not in $\hat{S}$). The cost is an approximation of the average energy consumed over a walking cycle. The goal will be to minimize $\hat{J}(a)$, subject to searching over values of a that will (tend to) give an asymptotically stable closed loop. To do this, the optimization is done subject to constraints $c \leq 0$, where

$$\begin{aligned} c_1 &:= \hat{\omega}_1^- - 0.99\lambda(\hat{\omega}_1^-) \\ c_2 &:= ||y(\bar{t})|| \\ c_3 &:= |F_T/F_N| - \mu \\ c_4 &:= -\dot{z}_2^+, \end{aligned}$$

and $\bar{t}$ is such that $\theta_1(\bar{t}) = \frac{1}{2}\theta_1^d$. The first constraint imposes that there exists a point where $\lambda(\omega_1^-) > \omega_1^-$, helping to assure the existence of a fixed point. The second constraint assures that the finite time controller has converged before impact (so that Theorem 1 is applicable), and the last two constraints assure that the impact model is valid.

This problem was set up and solved in MATLAB using the constrained optimization function `constr`, from the Optimization ToolBox. The functions η_i^a were taken as

$$\eta_1^a(\theta_1) := a_1^0 + \cdots + a_1^3(\theta_1)^3 \tag{23}$$

$$\eta_2^a(\theta_1) := -\theta_1 + (a_2^0 + \cdots + a_2^3(\theta_1)^3) \times (\theta_1 + \theta_1^d) \times (\theta_1 - \theta_1^d). \tag{24}$$

The rather particular form of η_2^a was arrived at by imposing that $h_2^a(\theta_1^d) = h_2^a(-\theta_1^d) = 0$, which is the condition needed for the robot's legs to have equal length at impact. The initial and final values of the parameters are shown in Table I, along with the cost. Figure 5 presents the corresponding graph of λ for the optimized value of the output functions. It is seen that there is an asymptotically stable orbit at $\omega_1^- \approx 1.56$. Simulation results support this. Figures 6 and 7 present the corresponding plots of θ and u, respectively, over a few cycles near the stable orbit. Fortuitously, the peak torque magnitude has been reduced to 85 Nm, without explicitly taking this as an objective in the optimization. Finite-time feedbacks with explicit magnitude constraints can also be designed; see [1].

Acknowledgments

This work was undertaken while J.W. Grizzle was on sabbatical leave at GRAVIR-LSIIT; he thanks Professor E. Ostertag for his kind hospitality. The work of J.W. Grizzle was supported in part by an NSF GOALI grant, ECS-9631237, and in part by matching funds from Ford Motor Company.

References

[1] S.P. Bhat and D.S. Bernstein. Continuous finite-time stabilization of the translational and rotational double integrators. *IEEE Transactions on Automatic Control*, 43(5):678–682, 1998.

[2] S.P. Bhat and D.S. Bernstein. Finite-time stability of continuous autonomous systems. *Preprint*, 1998.

[3] M. Bühler, D. E. Koditschek, and P. J. Kindlmann. Planning and control of a juggling robot. *International Journal of Robotics Research*, 13(2):101–118, 1994.

[4] M. Bühler, D. E. Koditschek, and P.J. Kindlmann. A family of robot control strategies for intermittent dynamical environments. *IEEE Control Systems Magazine*, 10(2):16–22, 1990.

[5] C. Canudas, L. Roussel, and A. Goswani. Periodic stabilization of a 1-dof hopping robot on nonlinear compliant surface. In *Proc. of IFAC Symposium on Robot Control*, pages 405–410, Nantes, France, September 1997.

[6] C. Chevallereau, A. Formal'sky, and B. Perrin. Control of a walking robot with feet following a reference trajectory derived from ballistic motion. In *Proc. of the IEEE International Conference on Robotics and Automation*, pages 1094–1099, Albuquerque, N.M., April 1997.

[7] B. Espiau and A. Goswani. Compass gait revisited. In *Proc. of the IFAC Symposium on Robot Control*, pages 839–846, Capri, Italy, September 1994.

[8] C. Francois and C. Samson. A new approach to the control of the planar one-legged hopper. *The International Journal of Robotics Research*, 17(11):1150–1166, 1998.

[9] J. Furusho and M. Masubuchi. Control of a dynamical biped locomotion system for steady walking. *Journal of Dynamic Systems, Measurement and Control*, 108:111–118, 1986.

[10] A. Goswani, B. Espiau, and A. Keramane. Limit cycles and their stability in a passive bipedal gait. In *Proc. of the IEEE International Conference on Robotics and Automation*, pages 246–251, Minneapolis, MN., April 1996.

[11] J.W. Grizzle, G. Abba, and F. Plestan. Asymptotically stable walking for biped robots: Analysis via systems with impulse effects. *Submitted to IEEE Transactions on Automatic Control*, Pre-print 1999.

[12] V.T. Haimo. Finite time controllers. *SIAM J. Control and Optimization*, 24(4):760–770, 1986.
[13] Y. Hurmuzlu. Dynamics of bipedal gait - part 1: objective functions and the contact event of a planar five-link biped. *Journal of Applied Mechanics*, 60:331–336, June 1993.
[14] Y. Hurmuzlu and D.B. Marghitu. Rigid body collisions of planar kinematic chains with multiple contact points. *The International Journal of Robotics Research*, 13(1):82–92, 1994.
[15] A. Isidori. *Nonlinear Control Systems: An Introduction*. Springer-Verlag, Berlin, 2nd edition, 1989.
[16] S. Kajita and K. Tani. Experimental study of biped dynamic walking in the linear inverted pendulum mode. In *Proc. of the IEEE International Conference on Robotics and Automation*, pages 2885–2891, Nagoya, Japan, May 1995.
[17] S. Kajita, T. Yamaura, and A. Kobayashi. Dynamic walking control of biped robot along a potential energy conserving orbit. *IEEE Transactions on Robotics and Automation*, 8(4):431–437, August 1992.
[18] D.D. Koditschek and M. Buhler. Analysis of a simplified hopping robot. *The International Journal of Robotics Research*, 10(6):587–605, 1991.
[19] N. Manamani, N.N. Gauthier, and N.K. M'Sirdi. Sliding mode control for pneumatic robot leg. In *Proc. of the European Control Conference*, Bruxelles, Belgium, July 1997.
[20] T. Marino and P. Tomei. *Nonlinear Control Design*. Prentice Hall, London, 1995.
[21] T. McGeer. Passive dynamic walking. *The International Journal of Robotics Research*, 9(2):62–82, 1990.
[22] J. Nakanishi, T. Fukuda, and D.E. Koditschek. Preliminary studies of a second generation brachiation robot controller. In *Proc. of the IEEE International Conference on Robotics and Automation*, pages 2050–2056, Albuquerque, N.M., April 1997.
[23] H. Nijmeijer and van der Schaft,A. J. *Nonlinear Dynamical Control Systems*. Springer-Verlag, Berlin, 1989.
[24] J.H. Park and K.D. Kim. Biped robot walking using gravity-compensated inverted pendulum mode and computed torque control. In *Proc. of the IEEE International Conference on Robotics and Automation*, pages 3528–3533, Leuven, Belgium, May 1998.
[25] J. Pratt and G. Pratt. Intuitive control of a planar bipedal walking robot. In *Proc. of the IEEE International Conference on Robotics and Automation*, pages 2014–2021, Leuven, Belgium, May 1998.
[26] M.H. Raibert, S. Tzafestas, and C. Tzafestas. Comparative simulation study of three control techniques applied to a biped robot. In *Proc. of the IEEE International Conference on Systems, Man and Cybernetics Systems Engineering in the Service of Humans*, pages 494–502, Le Touquet, France, October 1993.
[27] A. Sano and J. Furusho. Realization of natural dynamic walking using the angular momentum information. In *Proc. of the IEEE International Conference on Robotics and Automation*, pages 1476–1481, Cincinnati, OH., May 1990.
[28] U. Saranli, W.J. Schwind, and D.E. Koditschek. Toward the control of a multi-jointed, monoped runner. In *Proc. of the IEEE International Conference on Robotics and Automation*, pages 2676–2682, Leuven, Belgium, May 1998.
[29] C.L. Shih and W.A. Gruver. Control of a biped robot in the double-support phase. *IEEE Transactions on Systems, Man, and Cybernetics*, 22(4):729–735, 1992.
[30] A.C. Smith and M.D. Berkemeier. The motion of a finite-width wheel in 3d. In *Proc. of the IEEE International Conference on Robotics and Automation*, pages 2345–2350, Leuven, Belgium, May 1998.
[31] M.W. Spong and M. Vidyasagar. *Robot dynamics and control*. John Wiley and Sons, New York, 1989.
[32] B. Thuilot, A. Goswani, and B. Espiau. Bifurcation and chaos in a simple passive bipedal gait. In *Proc. of the IEEE International Conference on Robotics and Automation*, pages 792–798, Albuquerque, N.M., April 1997.
[33] M. Vukobratovic, B. Borovac, D. Surla, and D. Stokic. *Biped locomotion*. Springer-Verlag, Berlin, 1990.

VII. Appendix

Biped Swing Phase Model

$$\begin{aligned} L &= (\tfrac{5}{8}m + M_H)r^2{\omega_1}^2 + \tfrac{1}{8}mr^2{\omega_2}^2 + \tfrac{1}{2}M_T l^2{\omega_3}^2 - \tfrac{1}{2}mr^2\omega_1\omega_2\cos(-\theta_1+\theta_2) \\ &\quad + M_T r l\omega_1\omega_3\cos(-\theta_1+\theta_3) - g(\tfrac{3}{2}m + M_H + M_T)r\cos(\theta_1) + \tfrac{1}{2}gmr\cos(\theta_2) - gM_T l\cos(\theta_3) \end{aligned} \tag{25}$$

The matrix B is given by

$$B = \begin{bmatrix} -1 & 0 \\ 0 & -1 \\ 1 & 1 \end{bmatrix}. \tag{26}$$

Biped Impact Model

$$\begin{aligned} \omega_1^+(x) &= \frac{1}{\text{den}}\left[m\omega_1 - (4m + 4M_H + 2M_T)\omega_1\cos(2\theta_1 - 2\theta_2) + 2M_T\omega_1\cos(2\theta_1 - 2\theta_3) + 2m\omega_2\cos(\theta_1 - \theta_2)\right] \\ \omega_2^+(x) &= \frac{1}{\text{den}}\left[2M_T\omega_1\cos(-\theta_1 + 2\theta_3 - \theta_2) - (2m + 4M_H + 2M_T)\omega_1\cos(\theta_1 - \theta_2) + m\omega_2\right] \\ \omega_3^+(x) &= \frac{1}{l\,\text{den}}\left[(2mr + 2M_H r + 2M_T r)\omega_1\cos(\theta_3 + \theta_1 - 2\theta_2) - 2M_H r\omega_1\cos(-\theta_1 + \theta_3)\right. \\ &\quad -(2mr + 2M_T r)\omega_1\cos(-\theta_1 + \theta_3) + mr\omega_1\cos(-3\theta_1 + 2\theta_2 + \theta_3) - rm\omega_2\cos(-\theta_2 + \theta_3) \\ &\quad \left.-(3ml + 4M_H l + 2M_T l)\omega_3 + 2ml\omega_3\cos(2\theta_1 - 2\theta_2) + 2M_T l\omega_3\cos(-2\theta_2 + 2\theta_3)\right] \\ \text{den} &= -3m - 4M_H - 2M_T + 2m\cos(2\theta_1 - 2\theta_2) + 2M_T\cos(-2\theta_2 + 2\theta_3) \end{aligned}$$

TABLE I

RESULT OF OPTIMIZING THE CHOICE OF OUTPUTS FOR MINIMAL ENERGY CONSUMPTION.

i	a_0^i	a_1^i	a_2^i	a_3^i	$\hat{J}$
Original Values					
1	0.523	0	0	0	1,360
2	0	0	0	0	
Optimized Values					
1	0.512	0.073	0.035	-0.819	761
2	-2.27	3.26	3.11	1.89	

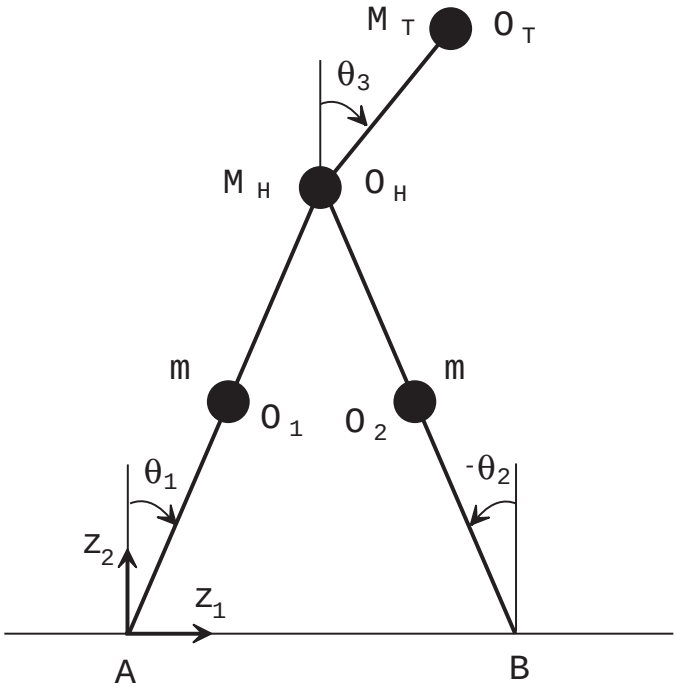

Fig. 1. Schematic indicating the definition of the generalized coordinates and the mechanical data of the biped robot. All masses are lumped. The legs are symmetric, with length r equal to the length of the line segment $A - O_H$ (also, $B - O_H$). The mass of each leg is lumped at $r/2$. The distance from the center of gravity of the hips to the center of gravity of the torso, denoted by l, is the distance from O_H to O_T.

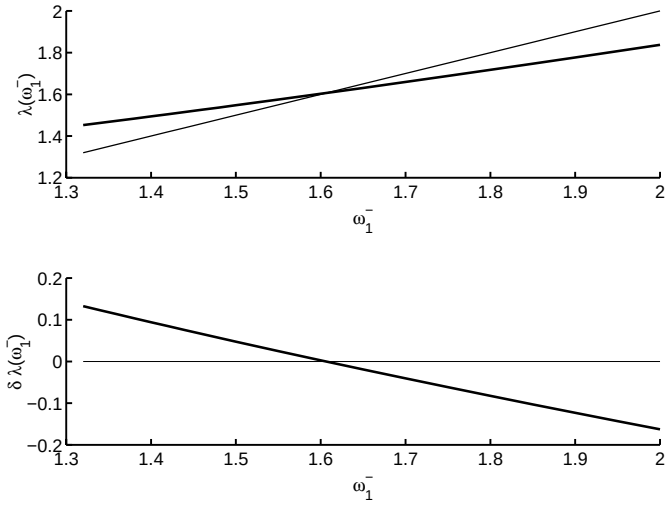

Fig. 2. The top graph presents the function λ (bold line) and, for visualization purposes, the identity function (thin line); the bottom graph presents the function $\delta\lambda$ (bold line) and the zero line (thin line). From either graph, it is seen that there exists a periodic orbit and that it is asymptotically stable.

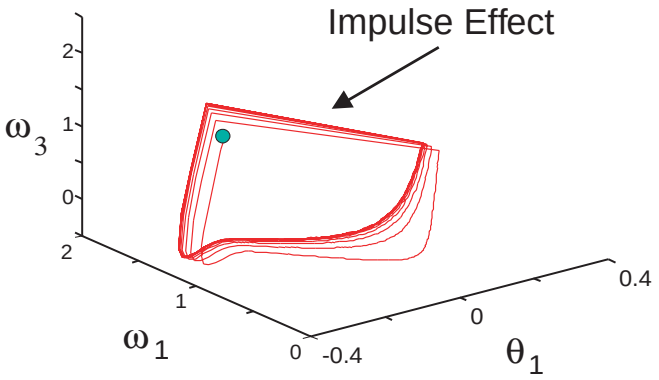

Fig. 3. An asymptotically stable orbit projected onto $(\theta_1, \omega_1, \omega_3)$.

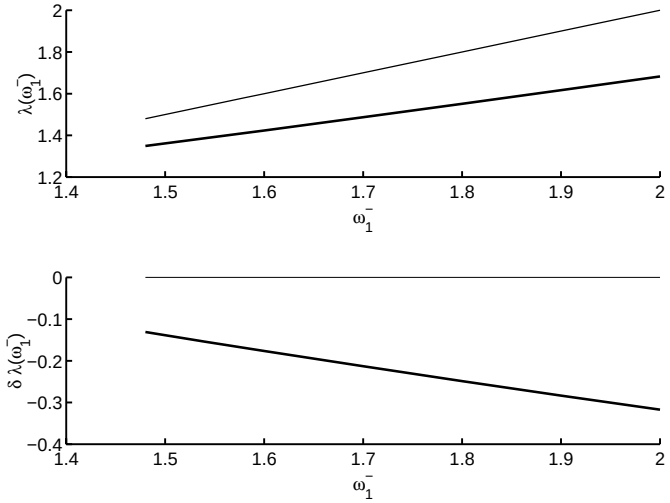

Fig. 4. The top graph presents the function λ (bold line) and, for visualization purposes, the identity function (thin line); the bottom graph presents the function $\delta\lambda$ (bold line) and the zero line (thin line). From either graph, it is seen that there does not exist a periodic orbit transversal to $\hat{S}$.

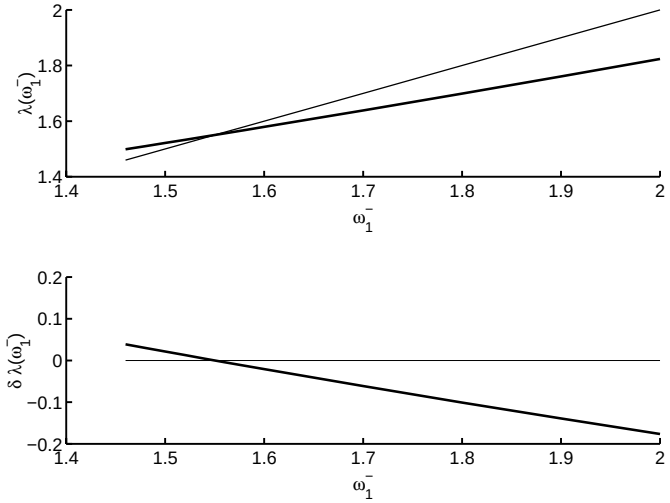

Fig. 5. The top graph presents the function λ (bold line) and, for visualization purposes, the identity function (thin line); the bottom graph presents the function $\delta\lambda$ (bold line) and the zero line (thin line). From either graph, it is seen that there exists a periodic orbit and that it is asymptotically stable.

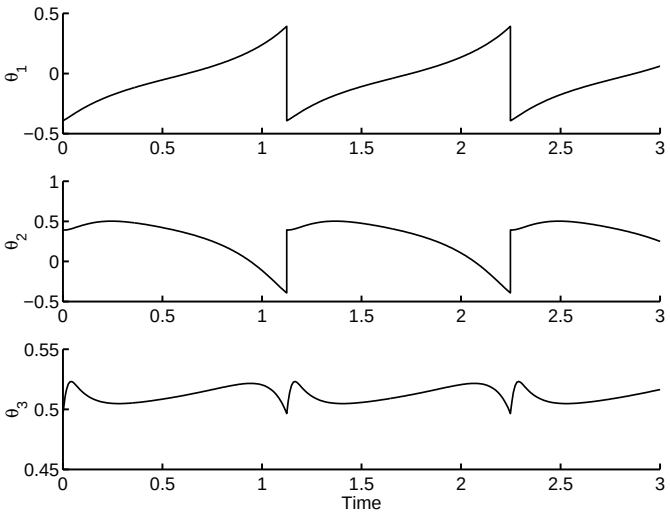

Fig. 6. Plot of joint angles versus time for a finite-time feedback computed on the basis of (23)-(24); units of radians.

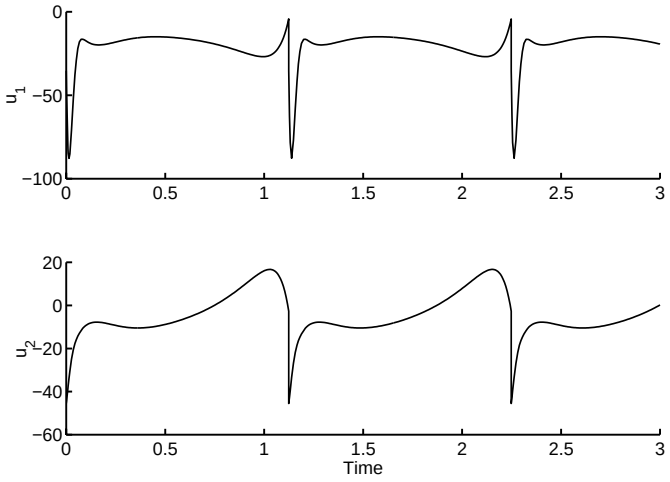

Fig. 7. Plot of applied torques versus time for a finite-time feedback computed on the basis of (23)-(24); units of newton-meters.